Some isomers and tautomers of goitrin – A DFT treatment

Lemi Türker

Department of Chemistry, Middle East Technical University, Üniversiteler, Eskişehir Yolu No: 1, 06800 Çankaya/Ankara, Turkey; e-mail: lturker@gmail.com; lturker@metu.edu.tr

Abstract

Goitrin is a molecule found in some goitrogenic plants. In the present study goitrin an its 1,3-proton tautomer, as well as the isomeric structures constructed by sulfur-oxygen replacement in the goitrin and its tautomer are considered within the restrictions of density functional theory at the level of B3LYP/6-31++G(d,p). All the structures considered presently are thermally favored and electronically stable at the standard states. On the other hand, in the presence of magnesium dication goitrin undergoes decomposition by the rapture of one of the C-O bonds. The effect of magnesium dication on the tautomer of goitrin is not so drastic but causes some conformational changes. Various geometrical and quantum chemical data have been collected and discussed, including IR and UV-VIS spectra.

1. Introduction

Thyroid hormones (thyroxine,T4; triiodothyronine,T3) play a vital role in the metabolism. In fetal life and throughout life they influence metabolic processes in almost all tissues. Thyroid gland which produces and stores these hormones requires iodide for hormone synthesis [1]. Naturally occurring goitrogens of the Brassicaceae family which includes cruciferous vegetables such as cabbage, brussels sprouts, kale, and turnips, utilizes a system made up of two main components: glucosinolates and myrosinase [2,3]. In the healthy plant, these are compartmentalized to prevent reaction. However, when the plant's tissues are damaged (e.g., by chewing), the compartments break down and the glucosinolates and myrosinase react, producing a burst of noxious secondary products that has been likened to a "bomb" [4] include cabbage, turnips rutabagas and mustards.

They contain progoitrins that become goitrogenic when acted upon by enzymes present in plant or in intestinal bacteria [2].

One of the most abundant products of glucosinolate–myrosinase reactions is goitrin (5-vinyloxazolidine-2-thione), which results from the hydrolysis of 2-hydroxy-3-butenyl glucosinolate (progoitrin) [5]. Goitrin is a potent inhibitor of thyroid peroxidase, which plays a central role in the organification of iodine [6]. Thus, consumption of goitrin interferes with thyroid hormone (TH) synthesis. Goitrin (5-vinyloxazolidine-2-thione), a potent antithyroid compound found naturally in crucifers. Individuals vary in ability to perceive synthetic compounds similar to goitrin, such as 6-propyl-2-thiouracil (PROP) and phenylthiocarbamide (PTC), as the result of mutations in the TAS2R38 gene, which encodes a bitter taste receptor.

Antiviral activity of certain herbs (like *Isatidis Radix*, root of *Isatis indigotica Fort.*) has drawn great attention due to its successful application in epidemics like severe acute respiratory syndrome (SARS) and avian influenza [7-9]. Results of in vivo studies indicated that epigoitrin ((+)-(R)-goitrin) was the therapeutic agent [10-12].

Although, the studies on goitrin go back to several decades ago, its popularity still remains in the scientific world [13-17]. However, to the best knowledge of the author no molecular orbital calculations exist in the literature on goitrin, its isomers and tautomers.

In the present study, (S)-5-vinyloxazolidine-2-thione,(goitrin) some of its isomers and tautomers are considered within the restrictions of density functional theory (DFT).

2. Method of Calculation

In the present study, the initial structural optimizations of all the structures leading to energy minima have been achieved by using MM2 method followed by semi-empirical PM3 self-consistent fields molecular orbital (SCF MO) method [18,19] at the restricted level [20,21]. Subsequent optimizations were achieved at Hartree-Fock level using various basis sets. Then, the structural optimizations were managed within the framework of density functional theory (DFT) [22,23] at the level of B3LYP/6-31++G(d,p) [21,24]. The exchange term of B3LYP consists of hybrid Hartree-Fock and local spin density (LSD) exchange functions with Becke's gradient correlation to LSD exchange [23,25]. The correlation term of B3LYP consists of the Vosko, Wilk, Nusair (VWN3) local correlation functional [26] and Lee, Yang, Parr (LYP) correlation correction functional [27]. Also, the vibrational analyses have been done. The total electronic energies are

corrected for the zero point vibrational energy (ZPE). The normal mode analysis for each structure yielded no imaginary frequencies for the $3N–6$ vibrational degrees of freedom, where N is the number of atoms in the system. This indicates that the structure of each molecule corresponds to at least a local minimum on the potential energy surface. All these calculations were done by using the Spartan 06 package program [28].

3. Results and Discussion

In the present study, goitrin and some of its isomers are considered. Of the four isomers of concern A and B are 1,3 tautomers of each other. Isomers C and D are also 1,3 tautomers of each other. Also presently goitrin (A) has been subjected to intra molecular perturbations doubly by interchanging the sulfur atom with oxygen atom keeping the bonding type be the same, thus the operation yields isomer-C and its tautomer D (see Figure 1). Note that of all four isomeric structures shown in the figure, A and B as well as C and D are pair wise tautomeric. Although, sulfur and oxygen atoms are in the same group, the possibility of valence shell expansion makes sulfur atom remarkable in certain respects.
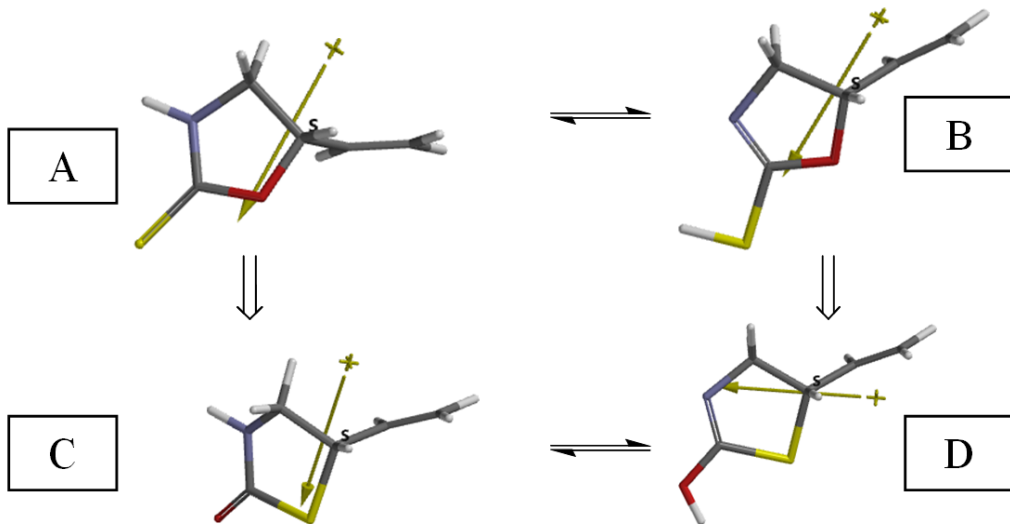

Figure 1. Optimized structures of the isomers considered.

Table 1 shows some of the thermo chemical data of the species considered. The data reveal that formations of the species are exothermic and favored. Note that A and B; C and D are tautomeric pairs and all four are isomers. The algebraic order of standard heat

of formation (Hº) values is C<A<B<D. The same order is valid for the Gibbs free energy of formations (Gº). According to the data, double centric perturbations on goitrin, namely exocyclic C=S to C=O and endocyclic -O- to -S- replacements, result in more exothermic structures. As for the respective tautomers the same sequence of perturbations lead to more exothermic structure having exocyclic -OH moiety compared to -SH. These trends dictate the Gº values leading to the mentioned order of favorability of the isomers or tautomers. Note that among the structures Sº values are comparable to each other and in magnitude they have of very small values compared to Hº and Gº.

Table 1. Some thermo chemical properties of the species considered.

Species	Hº	Sº (J/molº)	Gº
A	-1897687.921	349.11	-1897792.007
B	-1897649.790	355.17	-1897755.685
C	-1897742.051	350.61	-1897846.586
D	-1897666.515	354.05	-1897772.074

Energies in kJ/mol.

Table 2 shows some energies of the species considered where E, ZPE and E_C stand for the total electronic energy, zero point vibrational energy and the corrected total electronic energy, respectively. As the data reveal, all of the structures are electronically stable. The stability order is C<A<D<B. As seen in the table the perturbed species are more stable than the parent structures. The perturbations affect not only the electronic as well as the geometrical effectors (gross and fine topologies, sizes of the atoms, etc.). Structure-C is more favored and more stable than its parent structure-A (goitrin). In both of the cases the ring is somewhat slightly puckered. It is note worthy that the bond angle C4O1C2 in goitrin (A) is 110.43° whereas in C, it is (C4S3C2) 92.17° (see Figure 2 for numbering of the atoms). The N1C4O1 angle of structure-A is 108.47° but in structure-C N1C4S3 angle is 108.85°. In structure-A, O1C2C3C5 dihedral angle is -121.58°, whereas structure-C possesses S3C2C3C5 dihedral angle of -118.47°. The interaction between the lone-pairs of oxygen or sulfur atom with the ethylenic π-orbitals through space should be effective as well. The combination of all the geometrical effectors dictates the order of stabilities obtained presently.

Table 2. Some energies of the species considered.

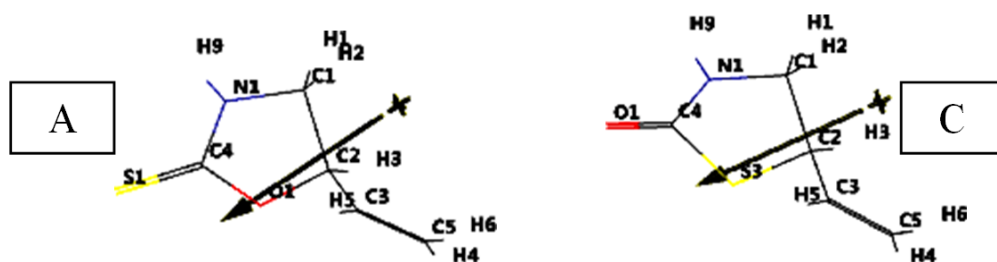| Species	E	ZPE	E_C
A	-1897999.52	308.44	-1897691.08
B	-1897952.77	298.91	-1897653.86
C	-1898052.78	307.10	-1897745.68
D	-1897975.38	304.45	-1897670.93

Energies in kJ/mol.

Figure 2. Numbering of atoms in structures-A and C.

Table 3 displays some calculated properties of these species. As seen in the table the presence of exocyclic double sulfur (structure A) or oxygen (structure C) atoms raises up the magnitude of the dipole moment values. Note that total dipole moment value is dictated by the magnitudes of the bond dipoles which are determined by both the

Table 3. Some properties of the species considered.

Species	Dipole moment	Polarizability	Ovality	Area (Å^2)	Volume (Å^3)	PSA (Å^2)
A	6.34	50.36	1.24	150.57	125.43	19.701
B	1.89	50.14	1.25	151.20	125.79	16.434
C	5.09	50.09	1.23	148.77	125.34	26.750
D	2.81	50.22	1.23	148.71	125.16	27.738

Dipole moments in debye units. Polarizabilities in 10^{-30} m^3 units.

electronic and geometrical factors (see Figures 1 and 3). Tautomers A,B or C,D have highly different dipole moment values. It is worth mentioning that the polar surface area (PSA) is defined as the amount of molecular surface area arising from polar atoms (N,O) together with their attached hydrogen atoms. Note that the high jump of PSA values of A to C or B to D. The polarizability is defined according to a multivariable formula which is a function of Van der Waals volume and hardness [28]. The later one is dictated by molecular orbital energies of the highest occupied (HOMO) and the lowest unoccupied (LUMO) molecular orbital energies.

Figure 3 displays the electrostatic potential (ESP) and the natural charges of the species considered. It is to be noted that the ESP charges are obtained by the program based on a numerical method that generates charges that reproduce the electrostatic potential field from the entire wavefunction [28].
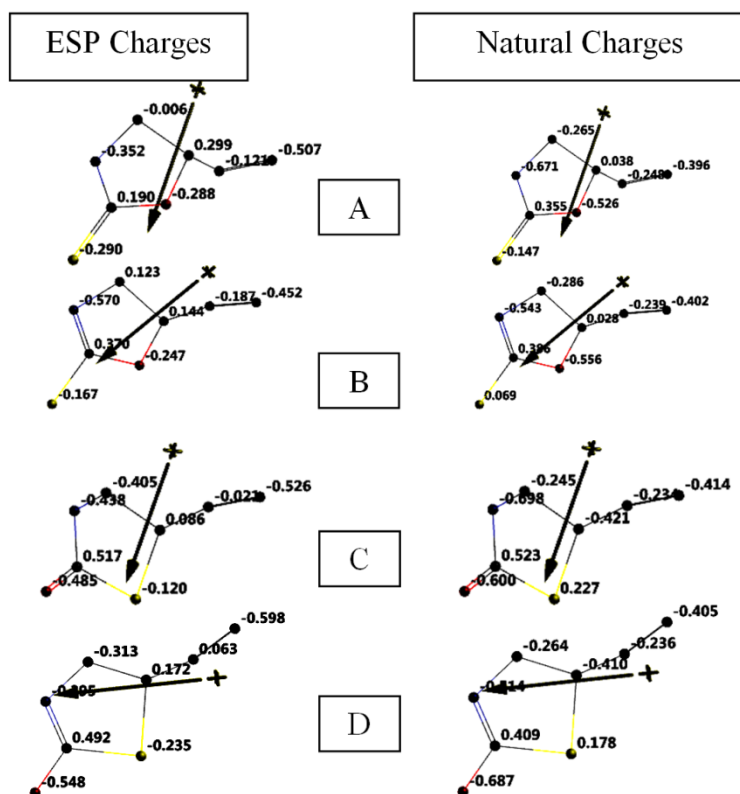

Figure 3. The ESP and natural charges on atoms of the species considered (Hydrogens not shown).

In the case of goitrin, the nitrogen atom linked to C=S moiety is more negative than the oxygen atom on the other side (both the ESP and natural charges). This is the case for the tautomer-B but in terms of the natural charges, the oxygen atom is slightly more negative. In the perturbed systems, both the ESP and natural charges have the same order of magnitudes like goitrin case, namely the nitrogen atom is more negative than the oxygen.

Figure 4 displays the electrostatic potential (ESP) maps of the species considered where negative potential regions reside on red/reddish and positive ones on blue/bluish parts of the maps.
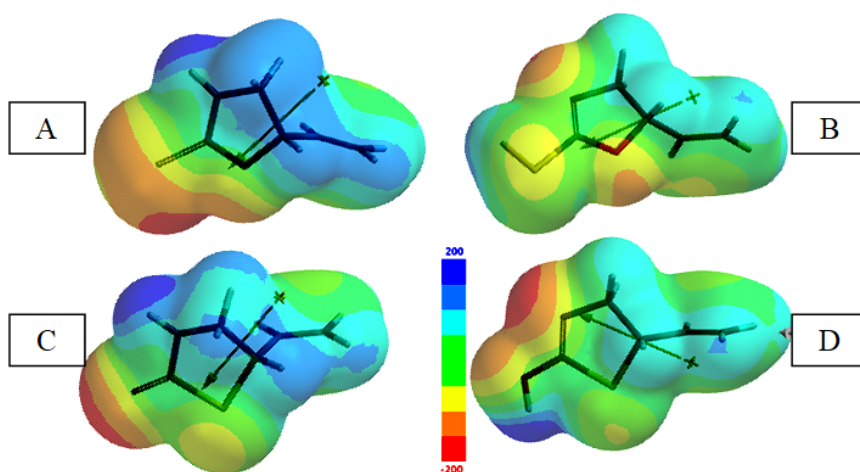

Figure 4. The ESP maps of the species considered.

Table 4 shows the aqueous and solvation energies for the species considered. The algebraic order of aqueous energies is C<A<D<B. On the other hand, the solvation energies follow the order of D<A<B<C. These orders are dictated by the presence of various chemical functional descriptors and their variations as going from one tautomer to the other or from one isomer to the other.

Table 4. Aqueous and solvation energies for the species considered.

	A	B	C	D
E_{aq}	-1898055.15	-1897989.35	-1898087.61	-1898040.08
Solvation energy	-55.628	-36.579	-34.832	-64.699

Energies in kJ/mol. SM5.4/A model used for solvation energy.

Figure 5 shows the chemical function descriptors (CFDs) of the species considered. Note that CFDs are attributes given to a molecule in order to characterize or anticipate its chemical behavior. In the figure the green, blue, purple and yellow colors stand for HBA; Hydrophobe; HBA, HBD, + ionizable; HBA, HBD types, respectively. The hydrogen bond acceptor and hydrogen bond donor characters are abbreviated as HBA and HBD, respectively.

As seen in the figure, some centers in the structures of the tautomers have completely changed their characters as compared to the respective ones in the parent structures. Also note the behavioral change of the stereogenic centers in tautomers B and D caused by the perturbation.
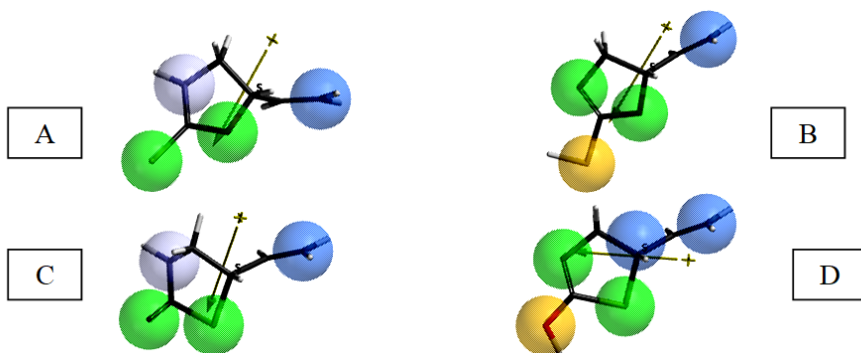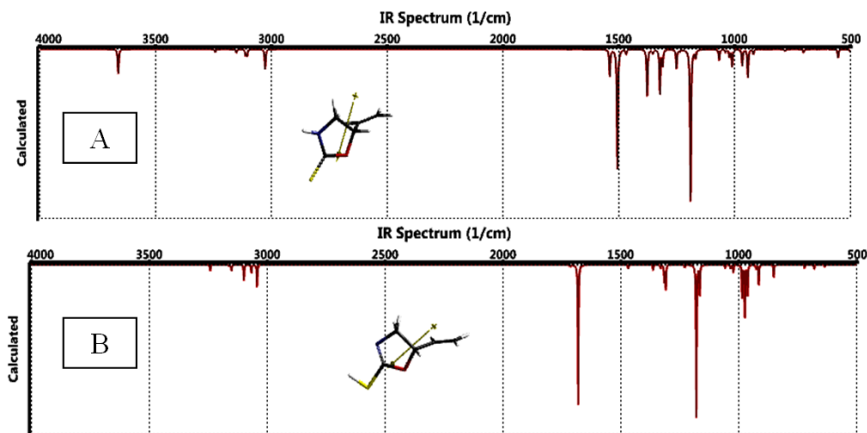

Figure 5. CFDs of the species considered.

Figure 6 displays the calculated IR spectra of the species considered and Table 5 lists some of the calculated stretchings frequencies. Various C-H stretchings occur between 3000-3500 cm^{-1}.
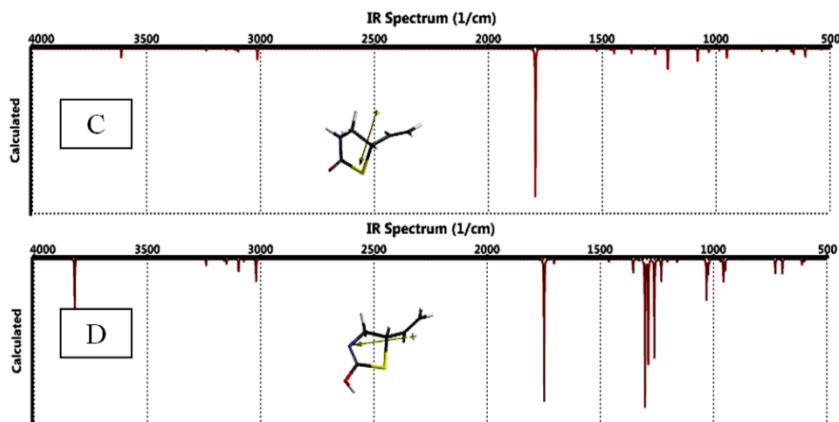
Figure 6. The calculated IR spectra of the species considered.

Table 5 also shows intensities of some of the selected stretching frequencies for the species considered.

Table 5. Some calculated stretchings frequencies.

Species	ν (cm$^{-1)}$	Intensity	Remark
A	3361	64.18	N-H
	1190	390.45	C=S
B	2735	0.01	S-H
	1180	256.08	C-S
C	3611	42.26	N-H
	1793	650.17	C=O
D	3821	82.90	O-H
	1231	35.58	C-O

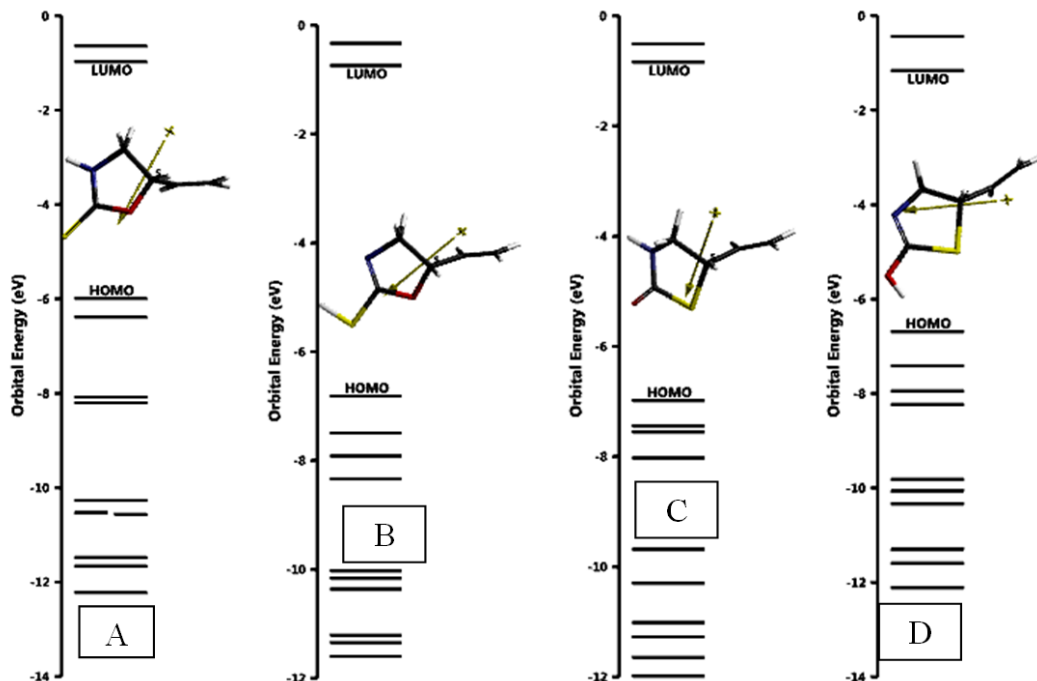Figure 7 shows some of the molecular orbital energy levels of the species considered.

Figure 7. Some of the molecular orbital energy levels of the species considered.

Table 6 lists the HOMO and LUMO (frontier molecular orbitals) energies and the interfrontier molecular orbital energy gap ($\Delta\varepsilon=\varepsilon_{LUMO}-\varepsilon_{HOMO}$) values of the molecules considered.

Table 6. The HOMO, LUMO energies and $\Delta\varepsilon$ values of the species considered.

Species	HOMO	LUMO	$\Delta\varepsilon$
A	-578.13	-93.60	484.53
B	-657.46	-71.15	586.31
C	-673.71	-81.19	592.52
D	-645.24	-111.57	533.67

Energies in kJ/mol.

Figure 8 displays the top views of the HOMO and LUMO patterns of the species considered. As seen in the figure, in the cases of structures-A and B, the ethylenic moiety

does not contribute in to the HOMO whereas in the perturbed cases, C and D, some contribution exist. Also note the large contribution of ring sulfur atom in the cases of C and D. As for the LOMOs, in every case the ethylenic moiety contributes a lot.

In general, the HOMO and LUMO (frontier molecular orbitals) are the most important orbitals in various chemical reactions and their energies are the effective ones on the kinetics of those reactions [29]. On the other hand, NEXTHOMO and NEXTLUMO may become important in secondary orbital interactions which might be decisive on regio and stereo selectivity of reactions [29]. Figure 9 shows the NEXTHOMO (HOMO-1) and NEXTLUMO (LUMO+1), patterns of species-A and -C considered.
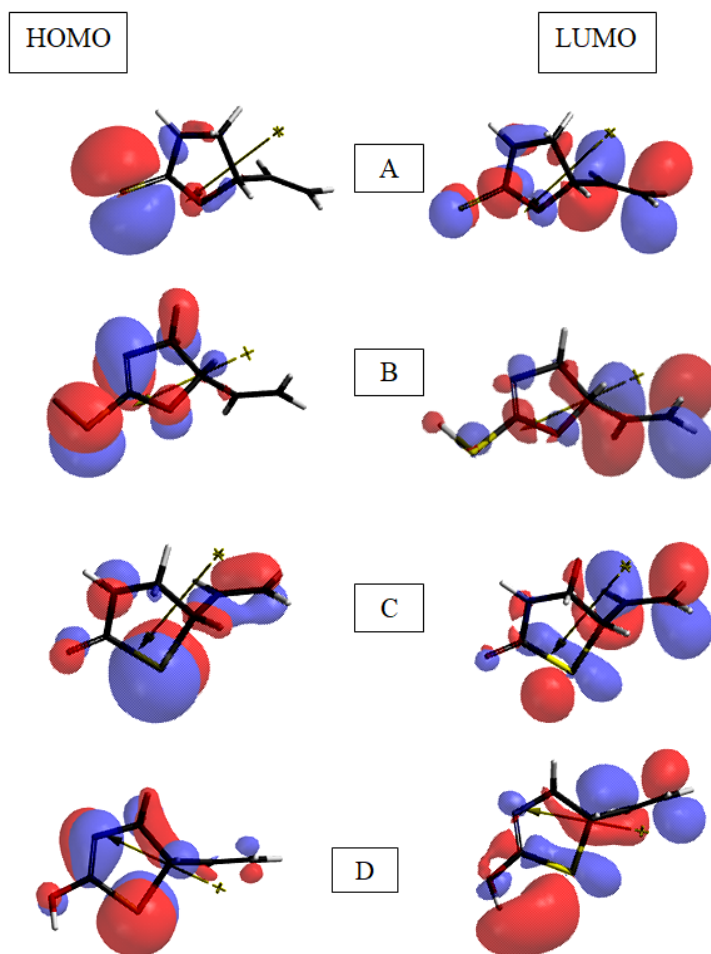

Figure 8. The HOMO and LUMO patterns of the species considered.
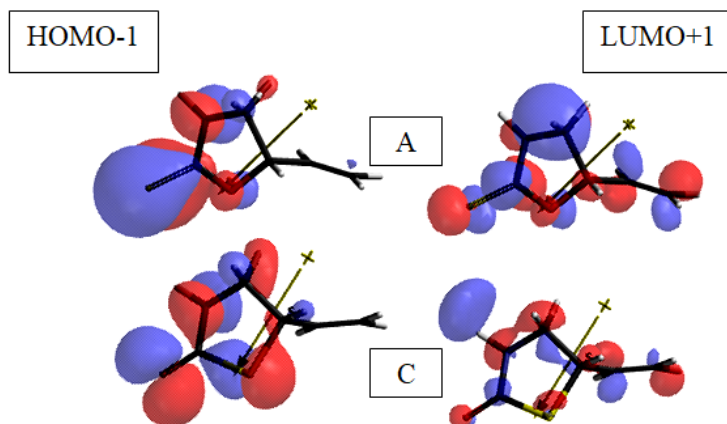
Figure 9. The NEXTHOMO and NEXTLUMO patterns of the species-A and -C considered.

Figure 10 shows the calculated (time dependent DFT) UV-VIS spectra of the isomers considered. As seen in the figure, they all absorb in the UV region having no absorbance in the visible part. The lack of any extended conjugation involving both the ring and the ethylenic chromophore should be the reason.
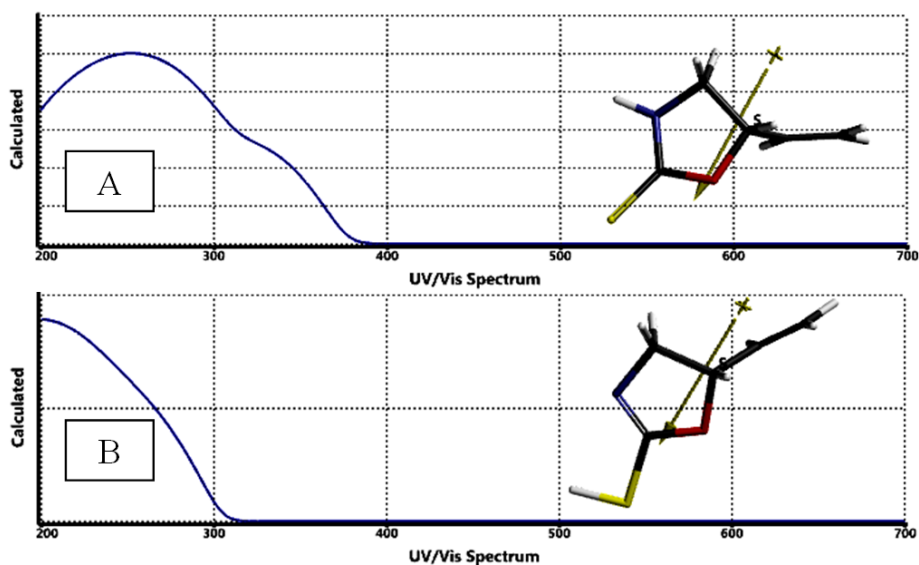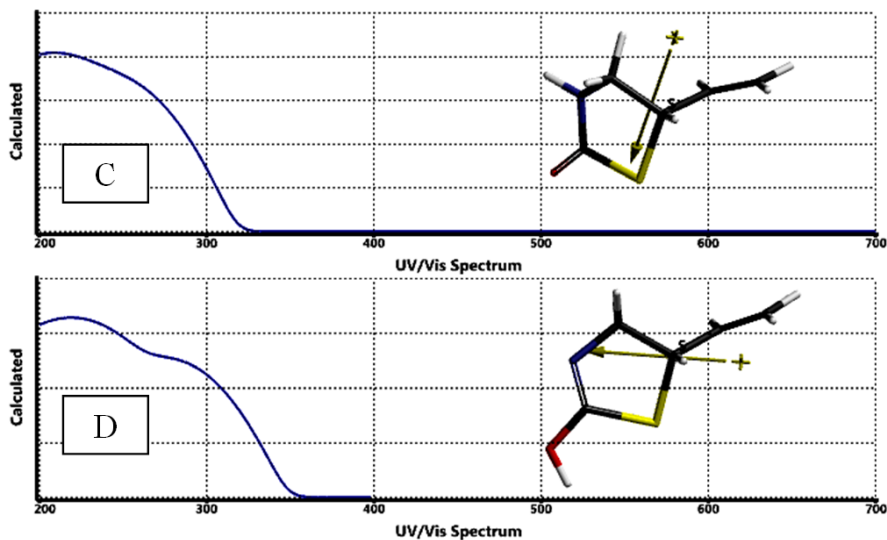
Figure 10. The calculated UV-VIS spectra of the species considered.

Effect of Mg^{+2} on goitrin and its tautomer

In this section effect of Mg^{+2} on goitrin (A) and its tautomer (B) has been investigated. Magnesium, in the cationic form or as many complexes, is one of the important elements in the biological processes. Figure 11 shows the optimized structures of the magnesium composites of goitrin, structure-A, and its tautomer, structure-B (see also Figure 1).

Figure 11. The optimized structures of goitrin and its tautomer in the presence of magnesium dication.

As seen in the figure, the magnesium dication causes decomposition of goitrin. The interaction of the cation is mainly with the oxygen atom, not with the sulfur or the nitrogen. The elongated O-C bond of the S=C-O moiety is 2.72 Å. The effect of the cation on tautomer-B is a conformational change only and no rapture of any bonds occurs. Figure 12 shows the ESP charges on atoms of the composite species considered

(Hydrogens not shown). In both of the composites, the magnesium, initially in dication form gets some electron population from the organic partner to reduce its charge. However, this reduction process of the cation (or oxidation of the organic participant) takes place better in the case of tautomer-B without decomposition and it seems more electron population has been transferred to the cation and decreasing its charge more. Note that the interaction energy which determines the outcome of many regio- and site selectivity issues is dictated by charge-based and/or orbital-based factors at different extents.
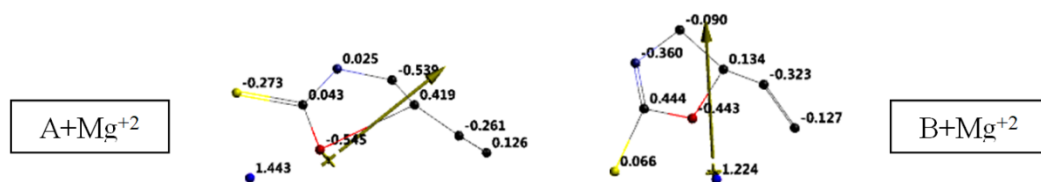

Figure 12. The ESP charges on atoms of the composite species considered (Hydrogens not shown).

The data presented in Table 7 reveal that the decomposed product has more exothermic heat of formation and more favorable G^o values at the standard states compared to B+ Mg^{+2} case.

Table 7. Some thermo chemical properties of the composite species considered.

Species	H^o	S^o (J/mol^o)	G^o
A+ Mg^{+2}	-2421469.012	386.31	-2421584.191
B+ Mg^{+2}	-2421304.722	374.94	-2421416.512

Energies in kJ/mol.

Table 8 shows some energies of the composite species considered. The decomposition leads to an energetically more stable form compared to the B+ Mg^{+2} case in which the organic partner remains intact in the composite.

Table 8. Some energies of the composite species considered.

Species	E	ZPE	E_C
A+ Mg^{+2}	-2421779.54	307.58	-2421471.96
B+ Mg^{+2}	-2421608.95	302.27	-2421306.68

Energies in kJ/mol.

The HOMO, LUMO and Δε values of the composite species considered are shown in Table 9. The data in the table reveals that the decomposition results in higher HOMO but somewhat lower LUMO energies compared to the respective energies of B+ Mg^{+2} composite. Consequently, the order of interfrontier molecular orbital energy gaps turns into A+ Mg^{+2} < B+ Mg^{+2}.

Table 9. The HOMO, LUMO and Δε values of the composite species considered.

Species	HOMO	LUMO	Δε
A+ Mg^{+2}	-1418.17	-1184.89	233.28
B+ Mg^{+2}	-1598.40	-1179.20	419.20

Energies in kJ/mol.

Figure 13 shows distributions of some of the molecular orbital energy levels of the composites considered.
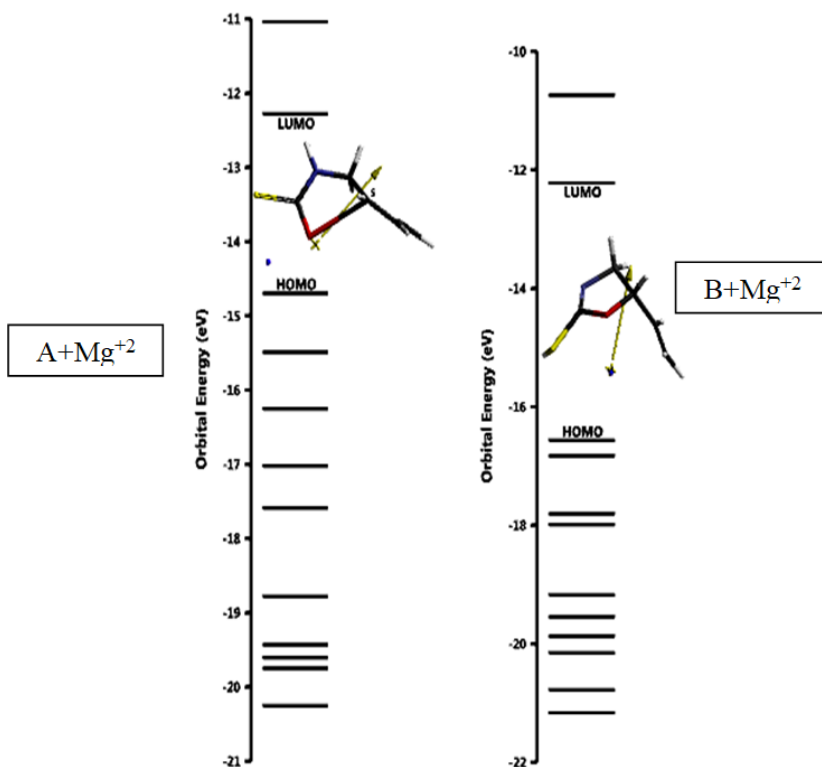

Figure 13. Some of the molecular orbital energy levels of the composites considered.

Figure 14 displays the calculated UV-VIS spectra (TDDFT) of the composites considered. Since, the calculated order of interfrontier molecular orbital energy gap is $A+ Mg^{+2} < B+ Mg^{+2}$, this fact should be the cause of apparent bathochromic shift in the UV-VIS spectrum of decomposed composite, $A+ Mg^{+2}$.
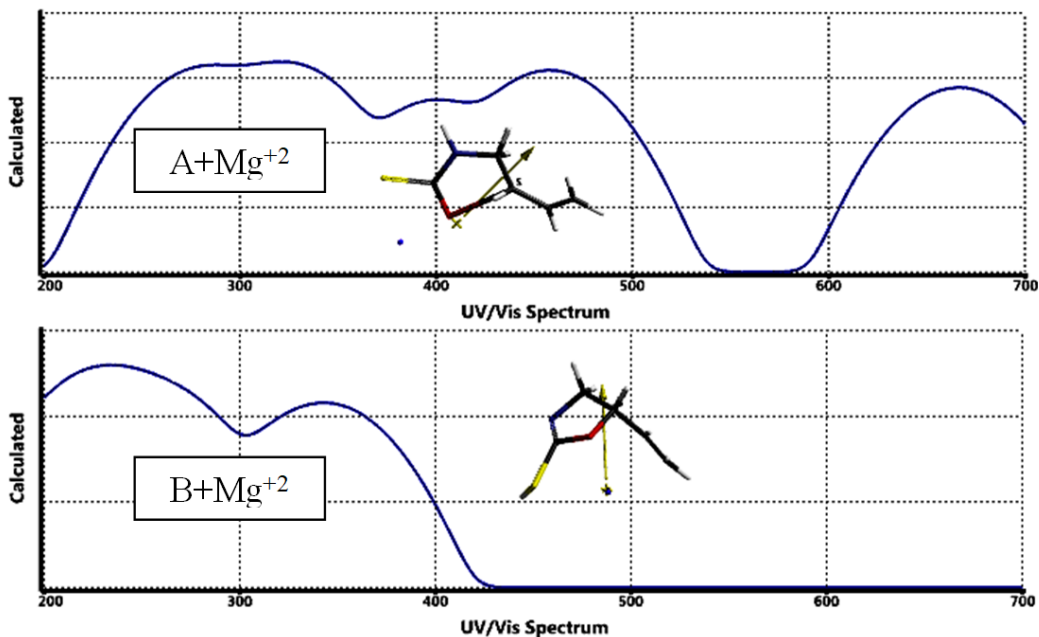

Figure 14. The calculated UV-VIS spectra of the composites.

4. Conclusion

In the present computational study, goitrin and its 1,3-proton tautomer, as well as the isomeric structures constructed by sulfur-oxygen replacement in the goitrin and its tautomer are considered within the restrictions of density functional theory. In the vacuum conditions, all of them are characterized with favorable Gibbs free energy of formation values and they are electronically stable. In the presence of Mg dication, goitrin undergoes decomposition by the cleavage of one of the C-O bonds while the goitrin tautomer remains structurally intact. However, one has to keep in mind that magnesium dication in aqueous medium is hydrated or complexed with some other anions present. Therefore, its oxidizing effect on goitrin might not be so great as it has been in the vacuum conditions.

References

[1] Greenspan, F.S., & Dong, B.J. (1984). *Thyroid and antithyroid drugs*, (in Basic and clinical pharmacology, Kanzung, B.G. (Ed.) (2nd ed.)). Los Altos, California: Lange Medical Pub.

[2] Greenspan, F.S., & Rapport, B. (1983). *Thyroid gland*, (in Basic and clinical endocrinology, Greenspan, F.S., & Horsham P.H. (Eds.)). Los Altos, California: Lange Medical Pub.

[3] Bones, A.M., & Rossiter, J.T. (1996). The myrosinase-glucosinolate system, its organization and biochemistry. *Physiologia Plantarum*, *97*, 194-208. https://doi.org/10.1111/j.1399-3054.1996.tb00497.x

[4] Kissen, R., Rossiter, J., & Bones, A. (2009). The 'mustard oil bomb': not so easy to assemble?! Localization, expression and distribution of the components of the myrosinase enzyme system. *Phytochem Rev.*, *8*, 69-86. https://doi.org/10.1007/s11101-008-9109-1

[5] Mithen, R. (2006). *Plant secondary metabolites: occurrence, structure, and role in the human diet. Sulfur-containing compounds*. (In: Crozier, A., Clifford, M.N., Asihara, H., (Eds.)). Oxford: Blackwell Publishing, Ltd. p. 25-46. https://doi.org/10.1002/9780470988558.ch2

[6] Gaitan, E. (1990). Goitrogens in food and water. *Annu Rev Nutr*. *10*, 21-39. https://doi.org/10.1146/annurev.nu.10.070190.000321

[7] Ke, L.J., Wen, T., Bradshaw, J.P., Zhou, J., & Rao, P. (2012). Antiviral decoction of *Isatidis Radix* inhibited influenza virus adsorption on MDCK cells by cytoprotective activity. *Journal of Traditional and Complementary Medicine*, *2*(1), 47-51. https://doi.org/10.1016/S2225-4110(16)30070-0

[8] Li, Q., Chen, J., Xiao, Y., Di, P., Zhang, L., & Chen, W. (2014). The dirigent multigene family in *Isatis indigotica*: gene discovery and differential transcript abundance. *BMC Genomics*, *15*, article 388. https://doi.org/10.1186/1471-2164-15-388

[9] Tian, L., & Wang, Z. (2012). Study on antibacterial activity of *Radix isatidis* extracts and preliminary investigation of their antibacterial mechanism. in *Proceedings of the 2012 International Conference on Applied Biotechnology*, Berlin, Germany: Springer.

[10] Xu, L.-H., Huang, F., Cheng, T., & Wu, J. (2005). Antivirus constituents of radix of *Isatis indigotica*. *Chinese Journal of Natural Medicines*, *3*(6), 359-360. http://zgtryw.periodicals.net.cn

[11]   Ye, W.Y., Li, X., & Cheng, W.J. (2011). Screening of eleven chemical constituents from *Radix Isatidis* for antiviral activity. *African Journal of Pharmacy and Pharmacology*, *5*(16), 1932-1936. https://doi.org/10.5897/AJPP11.559

[12]   Zhang, S.J., Liu, M.H., Li, H.B., Jiang, L., Luo, Y., & Sun, Q. (2013). In *vitro* anti-viral effects and dose-effect relationship of epigoitrin and fructopyrano-(1 → 4)-glucopyranose based on deletion/increment strategy. *Chinese Journal of New Drugs*, *22*(9), 1083-1087.

[13]   Felker, P., Bunch, R., & Leung, A.M. (2016). Concentrations of thiocyanate and goitrin in human plasma, their precursor concentrations in brassica vegetables, and associated potential risk for hypothyroidism. *Nutrition Reviews*, *74*(4), 248-258. https://doi.org/10.1093/nutrit/nuv110

[14]   Wooding, S., Gunn, H., Ramos, P., Thalmann, S., Xing, C., & Meyerhof, W. (2010). Genetics and bitter taste responses to goitrin, a plant toxin found in vegetables. *Chemical Senses*, *35*(8), 685-692. https://doi.org/10.1093/chemse/bjq061

[15]   Xie, Z., Shi, Y., Wang, Z., Wang, R., & Li, Y. (2011). Biotransformation of glucosinolates epiprogoitrin and progoitrin to (R)- and (S)-goitrin in Radix isatidis. *J. Agric. Food Chem., 59* (23), 12467-12472. https://doi.org/10.1021/jf203321u

[16]   Nie, L., Dai, Z., & Ma, S. (2016). Improved chiral separation of (R,S)-goitrin by SFC: An application in traditional chinese medicine. *Journal of Analytical Methods in Chemistry*, *2016*, 5782942. https://doi.org/10.1155/2016/5782942

[17]   Nie, L., Wang, G., Dai, Z., & Lin, R. (2010). Determination of epigoitrin and goitrin in *Isatidis Radix* by chiral high performance liquid chromatography. *Chinese Journal of Chromatography*, *28*(10), 1001-1004. http://dx.doi.org/10.3724/SP.J.1123.2010.01001

[18]   Stewart, J.J.P. (1989). Optimization of parameters for semiempirical methods I. Method. *J. Comput. Chem.*, *10*, 209-220. https://doi.org/10.1002/jcc.540100208

[19]   Stewart, J.J.P. (1989). Optimization of parameters for semi empirical methods II. Application. *J. Comput. Chem.*, *10*, 221-264. https://doi.org/10.1002/jcc.540100209

[20]   Leach, A.R. (1997). *Molecular modeling* (2nd ed.). Longman, Essex.

[21]   Fletcher, P. (1990). *Practical methods of optimization* (1st ed.). New York: Wiley.

[22]   Kohn, W., & Sham, L. (1965). Self-consistent equations including exchange and correlation effects. *J. Phys. Rev.*, *140*, 133-1138. https://doi.org/10.1103/PhysRev.140.A1133

[23]   Parr, R.G., & Yang, W. (1989). *Density functional theory of atoms and molecules* (1st ed.). London: Oxford University Press.

[24] Cramer, C.J. (2004). *Essentials of computational chemistry* (2nd ed.). Chichester, West Sussex: Wiley.

[25] Becke, A.D. (1988). Density-functional exchange-energy approximation with correct asymptotic behavior. *Phys. Rev. A*, *38*, 3098-3100. https://doi.org/10.1103/PhysRevA.38.3098

[26] Vosko, S.H., Wilk, L., & Nusair, M. (1980). Accurate spin-dependent electron liquid correlation energies for local spin density calculations: a critical analysis. *Can. J. Phys.*, *58*, 1200-1211. https://doi.org/10.1139/p80-159

[27] Lee, C., Yang, W., & Parr, R. G. (1988). Development of the Colle-Salvetti correlation energy formula into a functional of the electron density. *Phys. Rev.*, *B*, *37*, 785-789. https://doi.org/10.1103/PhysRevB.37.785

[28] SPARTAN 06, Wavefunction Inc., Irvine CA, USA, 2006.

[29] Fleming, I. (1976). *Frontier orbitals and organic reactions*. London: Wiley.